



## Models of Calmodulin Trapping and CaM Kinase II Activation in a Dendritic Spine

WILLIAM R. HOLMES

*Neurobiology Program, Department of Biological Sciences, Ohio University, Athens, OH 45701*

holmes@ohiou.edu

*Received November 11, 1998; Revised March 22, 1999; Accepted April 5, 1999*

Action Editor: Steve Redman

**Abstract.** Activation of calcium/calmodulin-dependent protein kinase II (CaMKII) by calmodulin following calcium entry into the cell is important for long-term potentiation (LTP). Here a model of calmodulin binding and trapping by CaMKII in a dendritic spine was used to estimate levels and durations of CaMKII activation following LTP-inducing tetani. The calcium signal was calcium influx through NMDA receptor channels computed in a highly detailed dentate granule cell model. Calcium could bind to calmodulin and calmodulin to CaMKII. CaMKII subunits were either free, bound with calmodulin, trapped, autonomous, or capped. Strong low-frequency tetanic input produced little calmodulin trapping or CaMKII activation. Strong high-frequency tetanic input caused large numbers of CaMKII subunits to become trapped, and CaMKII was strongly activated. Calmodulin trapping and CaMKII activation were highly dependent on tetanus frequency (particularly between 10 and 100 Hz) and were highly sensitive to relatively small changes in the calcium signal. Repetition of a short high-frequency tetanus was necessary to achieve high levels of CaMKII activation. Three stages of CaMKII activation were found in the model: a short, highly activated stage; an intermediate, moderately active stage; and a long-lasting third stage, whose duration depended on dephosphorylation rates but whose decay rate was faster at low CaMKII activation levels than at high levels. It is not clear which of these three stages is most important for LTP.

**Keywords:** LTP, CaM kinase II, calmodulin, calcium, dendritic spine, dentate, computational model, hippocampus, phosphorylation, autophosphorylation

### 1. Introduction

Long-term potentiation (LTP) is a modification of synaptic strength that has been extensively studied in the hippocampus. In the dentate and CA1 regions its induction depends on calcium influx through N-methyl-D-aspartate (NMDA) receptor channels (for reviews, see Malenka and Nicoll, 1993; Bliss and Collingridge, 1993). How much calcium enters depends strongly on the strength and frequency of the stimulus because of the voltage-dependence of the NMDA receptor channel (Mayer et al., 1984).

It has been proposed that the strength of the calcium signal may determine whether LTP or long-term depression (LTD) is induced at a synapse (Lisman, 1989). Modeling studies (Holmes and Levy, 1990; Zador et al., 1990) and experimental studies (Malenka, 1991; Hanse and Gustafsson, 1992) have lent support to the idea that a threshold level of calcium is needed to induce LTP. It has been more difficult to determine threshold levels for LTD, and the temporal pattern or frequency of calcium transients may be more important for LTD than the absolute calcium level (Cummings et al., 1996; Hansel et al., 1996).

Recent evidence suggests that a strong calcium signal may induce LTP by activating calcium/calmodulin-dependent protein kinase II (CaMKII) (for reviews, see Soderling, 1993; Fukunaga et al., 1996; Lisman, 1994; Lisman et al., 1997). Calcium entering the spine head can bind to calmodulin, and the calcium-calmodulin complex (CaM $\text{Ca}_4$ ) can bind to individual subunits of CaMKII and activate them. If enough subunits are activated, autophosphorylation may occur (Miller and Kennedy, 1986), which traps calmodulin on a subunit and makes the subunit active long after the calcium signal is over (Meyer et al., 1992). In the hippocampus it has been shown that a high-frequency stimulus, but not a low-frequency stimulus, can induce LTP with long-lasting increases in calcium-independent activity of CaMKII (Fukunaga et al., 1993). Mayford et al. (1995) have proposed that calcium-independent CaMKII activity levels may shift the threshold for the induction of LTP or LTD induced by tetanic stimulation. Recently, experimental evidence has been presented suggesting that the frequency and duration of calcium signals can be decoded into CaMKII activity levels (DeKoninck and Schulman, 1998). However, the frequency of calcium signals that would strongly activate CaMKII was much lower than the stimulation frequencies that are typically needed to induce LTP.

Models have been developed to gain an understanding of how calcium signals lead to calmodulin trapping and calcium-independent CaMKII activity (Dosemeci and Albers, 1996; Michelson and Schulman, 1994; Matsushita et al., 1995; Coomber, 1998). However, in these models the calcium signal was an arbitrary wave form, and the dynamics of calcium binding to calmodulin was not taken into account. In this article the calcium signal is obtained by computing calcium influx through NMDA receptor channels on dendritic spines following tetanic input to hundreds of synapses in a model of a fully reconstructed dentate granule cell. A model of calcium dynamics in a dendritic spine is used to determine levels of calmodulin loaded with four calcium ions (CaM $\text{Ca}_4$ ), and a stochastic model similar to that of Michelson and Schulman (1994) is used to estimate the extent of calmodulin trapping and calcium-independent CaMKII activity that may occur with different stimuli. These simulations relate stimulation frequency requirements to voltage and calcium signal requirements for different CaMKII activation levels in a dendritic spine. They reveal three distinct stages of CaMKII activation with high activation levels correlated with conditions that lead to LTP experimentally,

and they also reconcile the low calcium signal frequencies needed to strongly activate CaMKII with the much higher stimulation frequencies needed to induce LTP.

## 2. Methods

### 2.1. Cell Used in the Simulations

A fully reconstructed dentate granule cell was modeled with voltage-dependent conductances on the soma, axon, and proximal dendrites as described previously (Holmes and Levy, 1997). Strong excitation was modeled as activation of 300 excitatory synapses on dendritic spines in the middle third of the dendritic tree to represent strong medial perforant path (mpp) input. Weak excitation was modeled as activation of one synapse in the distal third of the dendritic tree representing weak lateral perforant path (lpp) input. These synapses were activated eight times at 10 to 400 Hz. Strong perforant path activation was assumed to activate a shunting inhibition in the distal two-thirds of the dendritic tree and at the soma. This powerful inhibition was modeled by reducing  $R_m$  in these regions from 40,000  $\Omega\text{cm}^2$  to 2,200  $\Omega\text{cm}^2$  (middle third and soma) or 1600  $\Omega\text{cm}^2$  (distal third) as suggested by Holmes and Levy (1997).

Non-NMDA and NMDA synaptic conductances were modeled on activated dendritic spines. The synaptic conductance time courses were determined from a model of glutamate release, diffusion, and binding to receptors (Holmes, 1995). The binding reactions included desensitization states and multiple closed states as shown in Holmes and Levy (1997). Peak conductance was not a model parameter in this study. For reference, the peak non-NMDA synaptic conductance following release of one vesicle of glutamate was approximately 140 pS, a value consistent with a number of experimental studies (e.g., Staley and Mody, 1991). Peak NMDA synaptic conductance in zero magnesium was slightly less than the single channel conductance or 50 pS. This value is lower than estimated by Bekkers and Stevens (1989) but is slightly higher than the average value estimated by Silver et al. (1993).

In modeling the 8 pulse tetanus, it was assumed that the probability of vesicle release was 1.0 for each pulse. However, several studies suggest that the probability of release is less than one (Hessler et al., 1993; Rosenmund et al., 1993; Walmsley et al., 1988). Furthermore, there may be facilitation of vesicle release

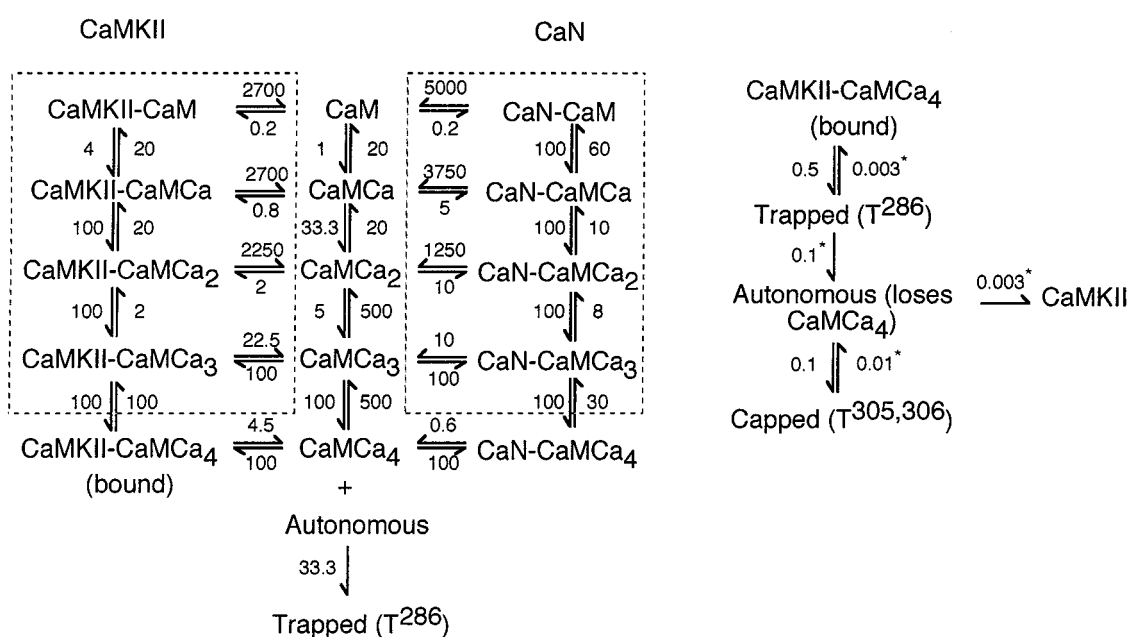


Figure 1. Calcium binding to calmodulin and subsequent reactions. Rate constants are given in  $\mu\text{M}^{-1}\text{s}^{-1}$  or  $\text{s}^{-1}$ . The reactions on the left were modeled deterministically, and the CaMKII subunit reactions (right) were modeled stochastically. The rate constants for the reactions in the dashed boxes are difficult to measure; these reactions were removed in some simulations. An asterisk next to a rate constant means that this rate constant was variable as described in the text.

among the first few pulses and depression later on as the readily releasable vesicle pool is depleted. These issues were not taken into account in the present study. Previous simulations found that calcium influx differed by only 10% for a 400 Hz, eight-pulse tetanus whether vesicle content was 2,000 or 10,000 (Holmes, 1995). This small difference occurred because, although release of one 2,000 molecule vesicle did not saturate receptors, multiple releases occurring with a high-frequency tetanus caused near-saturation of receptors. If a few of the pulses in the high-frequency tetanus do not cause vesicle release, there may still be enough glutamate released to cause near-saturation of receptors. Because of this, it was thought that not taking into account the stochastic nature of vesicle release would have a minimum impact on the qualitative features of the results presented here.

## 2.2. Dendritic Spine Model

The dendritic spine model was similar to that used previously (Holmes, 1990; Holmes and Levy, 1990, 1997), which calculated spine-head calcium concentration following calcium influx through NMDA receptor

channels while taking into account calcium diffusion, pumping and binding to buffers. The model had four spine-head compartments, four spine-neck compartments, and 12 dendritic compartments. The dendritic spine is assumed to be a long-thin spine with cylindrical dimensions  $d \times l$  of  $0.55 \times 0.55$  for the head and  $0.1 \times 0.73$  for the neck (Desmond and Levy, 1985). The major change to the model here is that reactions for calcium binding to calmodulin, calmodulin binding to CaMKII and calcineurin, and subsequent CaMKII transition steps were included as shown in Fig. 1. Initial calcium concentration was 70 nM. Calmodulin was assumed to be the only calcium buffer in this system. Calmodulin concentration is thought to lie between 10 and  $100 \mu\text{M}$  (Kakiuchi et al., 1982; Sharma et al., 1988) and the value used here was  $80 \mu\text{M}$ . Recent studies in muscle suggest that all but a small percentage of calmodulin is bound in the basal state (Luby-Phelps et al., 1995). It is not known if this is true in dendritic spines. Calmodulin with zero to four calcium ions could diffuse in the spine and dendrite with a diffusion coefficient assumed to be one-tenth that of calcium.

In most simulations CaMKII and calcineurin were assumed to be restricted to the outer 50 nm of the spine

head since CaMKII is a major component of the post-synaptic density (Kennedy et al., 1983; Kelly et al., 1984). There were 100 CaMKII molecules (each with 10 subunits that could bind CaM $\text{Ca}_4$ ) and 286 calcineurin molecules. In most simulations all CaM $\text{Ca}_x$  states could bind to CaMKII or calcineurin, but in a few simulations the reactions within the dashed boxes in Fig. 1 were eliminated and only the fully loaded calmodulin (CaM $\text{Ca}_4$ ) could bind to CaMKII or calcineurin. Calmodulin with less than four calcium ions bound can bind to substrates, but the data suggest that the affinity is likely to be substantially less than binding of calmodulin with four bound calcium ions (e.g., Gregori et al., 1985). Furthermore, enzymes do not seem to be activated by calmodulin that is not fully loaded with calcium (Crouch and Klee, 1980; Stull, 1988).

All steps involving calcium binding or calmodulin binding to CaMKII or calcineurin were computed deterministically from the differential equations associated with the binding reactions shown on the left in Fig. 1. Equations were solved with a fourth-order Runge-Kutta method with a 1.0  $\mu\text{s}$  time step. The steps involving CaMKII transitions from the bound to trapped, autonomous, or capped states shown on the right in Fig. 1 were computed stochastically with a method based on that of Michelson and Schulman (1994) with a 0.1 ms time step (extended to 0.1 seconds when calcium concentration had returned to rest). The justification for the separation of the reaction steps into deterministic and stochastic parts is that the transitions in these two parts of the model occur on vastly different time scales. Because of the variability inherent with stochastic simulations, each simulation was run four to 10 times, and the average results were calculated.

When [CaMKII-CaM $\text{Ca}_4$ ] in the outer 50 nm of the spine head was greater than the concentration of one molecule in that volume, the number of CaMKII-CaM $\text{Ca}_4$  subunits (bound) was computed. (When converting concentrations to numbers of molecules, the remaining fraction of a molecule was ignored.) If the number of bound subunits increased by  $x$  from the number at the previous time step, then  $x$  randomly selected free subunits were designated bound. If the number of bound subunits decreased by  $y$  from that at the previous time step, then  $y$  randomly selected bound subunits were designated free.

In the CaMKII subunit reactions a bound subunit could become trapped (CaM $\text{Ca}_4$  bound and phospho-

rylation at position T $^{286}$ ) only if its neighbor was also in the bound or trapped state (or with lower probability, in the autonomous or capped states, and with still lower probability, the free state). Trapping has been shown to be an intersubunit reaction (Hanson et al., 1994; Mukherji and Soderling, 1994), but it is not clear if there is directionality in the trapping. In the simulations the neighboring subunit involved in the trapping action could only be either the right-hand or left-hand neighbor. Having only the neighbor to the right involved in trapping, as in Michelson and Schulman (1994), reduced quantitatively the amount of trapping but had little qualitative effect on the results.

A trapped subunit becomes autonomous if CaM $\text{Ca}_4$  is released but the subunit remains phosphorylated at T $^{286}$ . A subunit cannot become autonomous from the free state without first being trapped since phosphorylation at T $^{286}$  is thought to require bound CaM $\text{Ca}_4$  (Hanson and Schulman 1992; Brickey et al. 1994).

Without CaM $\text{Ca}_4$  bound, phosphorylation can occur in autonomous subunits in the calmodulin binding site at T $^{305,306}$  taking the subunit into the capped state. This capping reaction has been shown to be an intersubunit reaction (Mukherji and Soderling 1994), but as with the trapping reaction, it is not known if this reaction is directional. In the simulations capping could occur only if the neighboring subunit to the right or left were bound, trapped, autonomous, or capped. Having only the neighbor to the right side involved in capping reduced quantitatively the amount of capping but had little qualitative effect on the results. The model assumes that free subunits cannot directly become capped because capped subunits are phosphorylated at T $^{286}$  and T $^{286}$  phosphorylation requires CaM $\text{Ca}_4$  binding as noted above.

The model does not include basal T $^{306}$  autophosphorylation in free subunits. This autophosphorylation occurs at a very slow rate, has a  $K_m$  value for ATP eightfold higher than CaM $\text{Ca}_4$  dependent autophosphorylation at T $^{286}$ , and causes the subunit to be inactivated (Colbran, 1993). If included in the model, the effect would be to remove a small number of subunits from consideration.

At each time step in the simulations, random numbers were chosen for each bound, trapped, autonomous, and capped subunit to determine which subunits would make transitions to which neighboring states. In some simulations the initial numbers of autonomous and capped subunits were nonzero to take into account a 4% to 20% basal activation of CaMKII subunits.

### 2.3. *Rationale for the Rate Constants Used: Deterministic Model*

**2.3.1. Calcium Binding to Calmodulin.** The rate constants for calcium binding to calmodulin (middle vertical reactions in Fig. 1) were chosen to satisfy the macroscopic binding constants for each step (20  $\mu\text{M}$ , 0.6  $\mu\text{M}$ , 100  $\mu\text{M}$ , and 5  $\mu\text{M}$ ) reported by Linse et al. (1991) and dissociation-rate data summarized by Klee (1988).

**2.3.2. Calcium Binding to Calcineurin-CaM $\text{Ca}_x$ .** These rate constants (right vertical reactions in Fig. 1) were chosen to satisfy the macroscopic binding constants for each step reported by Stemmer and Klee (1994) while assuming that the association rate constant was 100  $\mu\text{M}^{-1}\text{s}^{-1}$  (Kretsinger, 1991; and at the upper end of the range given by Linse and Forsen, 1995).

**2.3.3. Calcium Binding to CaMKII-CaM $\text{Ca}_x$ .** These rate constants (left vertical reactions in Fig. 1) are not known well. It was assumed that the rate constants were similar to calcium binding to calmodulin with the major difference occurring with the binding and unbinding of the third calcium ion as has been suggested for other calmodulin binding proteins (e.g., Burger et al., 1983, 1984; Cox et al., 1988).

**2.3.4. CaM-Ca $_x$  Binding to Calcineurin.** The dissociation constant for CaM $\text{Ca}_4$  binding to calcineurin has been reported to be 6 nM (Meyer et al., 1992). (Other reports give this dissociation constant at lower values, but model results were changed little by having this value at 0.1 nM because the 6 nM value was still much smaller than the value for binding to CaMKII as noted below.) With the binding rate constant assumed to be 100  $\mu\text{M}^{-1}\text{s}^{-1}$ , the unbinding rate was 0.6  $\text{s}^{-1}$ . For the other reactions (right horizontal reactions in Fig. 1), the macroscopic rate constants were chosen to satisfy thermodynamic equilibrium (that is, the product of the macroscopic rate constants from CaM $\text{Ca}_3$  to CaN-CaM $\text{Ca}_3$  to CaN-CaM $\text{Ca}_4$  equaled the product from CaM $\text{Ca}_3$  to CaM $\text{Ca}_4$  to CaN-CaM $\text{Ca}_4$ ) given the known macroscopic rate constants for calcium binding to CaM $\text{Ca}_x$  and CaM $\text{Ca}_4$  binding to calcineurin. Binding rates were assumed to be slow until three calcium ions had bound to calmodulin.

**2.3.5. CaM-Ca $_x$  Binding to CaMKII.** Meyer et al. (1992) report that the binding rate of dansylated

calmodulin saturated with calcium (with a fluorescent probe attached) is 0.15  $\mu\text{M}^{-1}\text{ms}^{-1}$ . Dansylated calmodulin has a threefold higher affinity for CaMKII than does unlabeled calmodulin. This difference could be exhibited in the binding rate, the unbinding rate, or both rates. A threefold lower binding rate would give a binding rate of 0.05  $\mu\text{M}^{-1}\text{ms}^{-1}$ . The assumption made here was that both rates would be affected, so the binding rate was chosen to be 0.1  $\mu\text{M}^{-1}\text{ms}^{-1}$  or 100  $\mu\text{M}^{-1}\text{s}^{-1}$ . The unbinding rate was computed from the binding rate and the dissociation constant for CaM $\text{Ca}_4$  binding to CaMKII assuming a value of 45 nM for the dissociation constant (Meyer et al., 1992). The result was 4.5  $\text{s}^{-1}$  for the unbinding constant. For the other reactions (left horizontal reactions in Fig. 1), the macroscopic rate constants were chosen to satisfy thermodynamic equilibrium with the major change again occurring with the binding of CaM $\text{Ca}_3$  to the protein. The computed macroscopic rate constants allowed almost no binding of calmodulin to CaMKII or calcineurin without at least two calcium ions bound to calmodulin for the calcium concentration levels achieved in the model.

**2.3.6. Autonomous to Trapped.** This transition occurs if CaM $\text{Ca}_4$  rebinds to an autonomous subunit. This binding rate was assumed to be one-third of the rate of CaM $\text{Ca}_4$  binding to CaMKII as suggested by Meyer et al. (1992), Table 1.

### 2.4. *Rationale for the Rate Constants Used: Stochastic Model*

The rate constants in Fig. 1 were converted into probabilities for the stochastic model by assuming that the probability of a transition in time interval  $\Delta t$  is  $1 - e^{-k\Delta t}$  for rate constant  $k$ . Since most rate constants were small, this quantity was usually equal to  $k\Delta t$ . Because many rate constants are not known very precisely, rate constants were varied 10-fold in some simulations.

**2.4.1. Bound to Trapped.** The bound-to-trapped rate constant depends on how fast autophosphorylation can occur. Autophosphorylation is an intersubunit reaction between neighboring subunits (Hanson et al., 1994) that occurs within 5 seconds in optimal conditions (Miller et al., 1988). Data from Hanson et al. (1994, figs. 5, 7) suggest 0.5 or 0.75  $\text{s}^{-1}$  would be an appropriate value although they used 5  $\text{s}^{-1}$  in their computer

model. Dosemeci and Albers (1996) used a value of  $0.05 \text{ s}^{-1}$  in their computer model. Here a rate constant of  $0.5 \text{ s}^{-1}$  was assumed if  $\text{CaMCA}_4$  was bound and the neighboring subunit was in the bound or trapped state. If the neighboring subunit were autonomous or capped, the rate constant was assumed to be  $0.5 \text{ s}^{-1}$  in most simulations but was reduced to  $0.2 \text{ s}^{-1}$  in some simulations to account for the reduced activity of subunits in the autonomous or capped states. If the neighboring subunit were not bound, trapped, autonomous, or capped, the rate constant was  $0.05 \text{ s}^{-1}$  to allow for phosphorylation to occur by chance encounter.

**2.4.2. Trapped to Autonomous.** The rate at which a trapped subunit becomes autonomous depends on calcium concentration as shown in Meyer et al. (1992, fig. 3). A function that fits the data in this figure is  $1/k = 0.00228 [\text{Ca}] 1.6919 + 9.88$ , where  $1/k$  is the inverse of the rate constant in seconds and calcium concentration is in nM. Given this function, the rate constant is  $0.1 \text{ s}^{-1}$  when  $[\text{Ca}^{2+}]$  is 10 nM but falls to  $0.00355 \text{ s}^{-1}$  when  $[\text{Ca}^{2+}]$  is  $1.0 \mu\text{M}$ .

**2.4.3. Autonomous to Capped.** The transition to the capped state is thought to be an intersubunit autophosphorylation (Mukherji and Soderling, 1994). This rate constant was assumed to be much slower than the bound to trapped rate constant. Basal autophosphorylation at  $\text{T}^{306}$  has been found to be about 25 times slower than  $\text{CaMCA}_4$  dependent phosphorylation at  $\text{T}^{286}$  (Colbran, 1993), but autophosphorylation at  $\text{T}^{306}$  may not be this slow if  $\text{T}^{286}$  is phosphorylated first. Data in Patton et al. (1990, fig. 5) suggest that a value of  $0.05\text{--}0.1 \text{ s}^{-1}$  would be appropriate and a value of  $0.1 \text{ s}^{-1}$  was used in most of the simulations when a neighboring subunit was bound, trapped, autonomous, or capped.

**2.4.4. Dephosphorylation Rates.** It was not known what the dephosphorylation rates should be or how these rates might change with calcium or calmodulin concentration. The base rate constant value used for  $\text{T}^{286}$  dephosphorylation was  $0.003 \text{ s}^{-1}$ . This is 10 times smaller than the rate used by Hanson et al. (1994). Data from Barnes et al. (1995) suggest that a larger value might be appropriate. Consequently, simulations were done with large variations in this parameter value. The capped to autonomous rate constant was assumed to

be threefold larger,  $0.01 \text{ s}^{-1}$ , as dephosphorylation at  $\text{T}^{305,306}$  was thought to proceed more quickly than at  $\text{T}^{286}$ . Data from Patton et al. (1990) suggest that under optimal conditions the rate could be up to 10-fold faster. Consequently, a large range of  $\text{T}^{305,306}$  dephosphorylation-rate constant values was tested. Although there is no evidence that calcineurin bound with  $\text{CaMCA}_4$  is directly responsible for the dephosphorylation of CaMKII subunits, it may have an indirect effect. Dephosphorylation rates were allowed to increase up to threefold depending on the proportion of calcineurin molecules that had  $\text{CaMCA}_4$  bound, delayed by 200 msec. Because of the small size of these rate constants, the threefold change had little quantitative effect on the results.

### 3. Results

Simulations were done first to determine whether high levels of calmodulin trapping on CaMKII were correlated with stimulation conditions thought to lead to LTP, including frequency and intensity requirements. Then, because CaMKII subunits are active in the autonomous and capped states, as well as the bound and trapped states, simulations were done to compare the time course of total CaMKII activation in stimulation conditions where LTP may or may not be induced. Finally, simulations were done to test how the time course of CaMKII activation might be affected with different parameter value choices, particularly for the dephosphorylation rates.

#### 3.1. High Levels of Calmodulin Trapping Correlated with Stimulation Conditions That Induce LTP

LTP is induced experimentally by strong high-frequency input but not by strong low-frequency input. Simulations were done to determine the amount of calmodulin trapping that occurs with a strong low frequency input. Three hundred excitatory synapses (representing medial perforant path input) were coactivated in the model once every 4 seconds (0.25 Hz). For this particular simulation, no shunting inhibition was included to maximize the amount of calmodulin trapping that might occur. Calcium concentration,  $\text{CaMCA}_4$  binding, and trapping on CaMKII were computed at a representative medial perforant path (mpp) synapse.

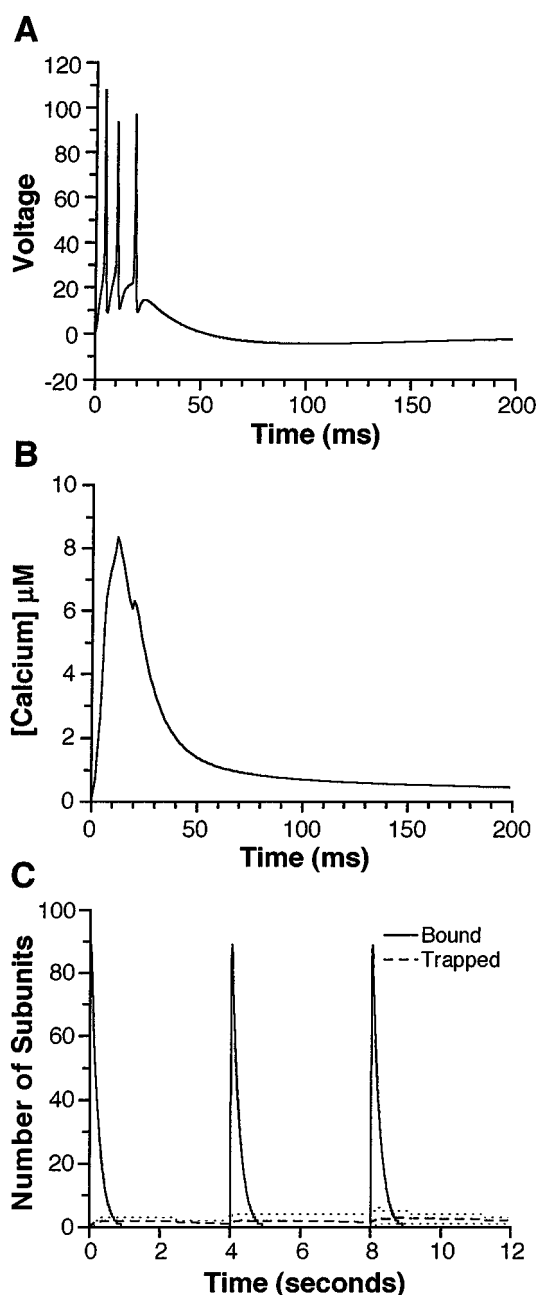


**Figure 2.** Almost no calmodulin trapping occurred for strong low frequency input. 300 mpp (excitatory) synapses were coactivated at 0.25 Hz. No inhibition was included in this simulation. **A:** Voltage response at the soma in mV. Voltage change is relative to the resting potential. **B:** Spine head calcium concentration at an mpp synapse. The notch in the plot was caused by action potential invasion of the dendritic spine containing the mpp synapse. **C:** Numbers of subunits of CaMKII that bound or trapped CaMCA<sub>4</sub>. The dotted lines for the number of trapped subunits represent the maximum and minimum numbers found in 10 runs of the stochastic simulation, whereas the dashed line is the average of 10 runs. Note the different time scale for this graph.

Almost no calmodulin trapping occurred with the strong low-frequency input. Because there was no inhibition, three action potentials were fired (Fig. 2A), and calcium concentration in the spine head peaked at more than 8  $\mu\text{M}$  (Fig. 2B). Despite this, very little CaMCA<sub>4</sub> became bound to CaMKII, and only two to three of the 1,000 subunits reached the trapped state (Fig. 2C).

Simulations were done with high-frequency tetanic input to determine the levels of calmodulin binding and trapping that occur with high-frequency input. Three hundred mpp synapses and one lateral perforant path (lpp) synapse were coactivated eight times at 400 Hz. The lateral perforant path synapse was added to allow the additional test of the “spatial convergence requirement” for associative LTP found in the dentate (White et al. 1988, 1990). For associative LTP to occur between coactivated weak and strong inputs to the dentate, the two inputs must converge in close spatial proximity to each other. Pairing strong medial perforant path input with weak lateral perforant path input will cause potentiation of mpp synapses but not of lpp synapses. A shunting inhibition, assumed to be activated by the tetanus, was included in the model. The tetanus was repeated every 4 seconds. Calcium concentration, CaMCA<sub>4</sub> binding, and trapping on CaMKII subunits were compared at a representative mpp synapse and the lpp synapse.

The amount of CaMCA<sub>4</sub> binding to CaMKII and CaMCA<sub>4</sub> trapping on CaMKII was much higher at the mpp synapse than at the lpp synapse and was much higher than that found above with low frequency input. Peak calcium concentration was twice as high at the mpp synapse than at the lpp synapse (Fig. 3A) and three times higher than in Fig. 2B. However, the difference in calcium concentration at the two synapses was small after the first 40 msec. Nevertheless, this twofold difference in peak calcium concentration led to twofold more CaMCA<sub>4</sub>-bound CaMKII subunits at the mpp synapse than at the lpp synapse (Fig. 3B) and threefold more subunits with CaMCA<sub>4</sub> trapped (Fig. 3C). At the peak of CaMCA<sub>4</sub> binding to CaMKII, 67% of the CaMKII subunits had CaMCA<sub>4</sub> bound at the mpp synapse, but only 36% of the subunits had CaMCA<sub>4</sub> bound at the lpp synapse. With the larger percentage of bound subunits at the mpp synapse, there was a higher probability that adjacent subunits were bound and that autophosphorylation to the trapped state would occur. This led to the threefold difference in the number of trapped subunits found between the mpp and lpp synapses.

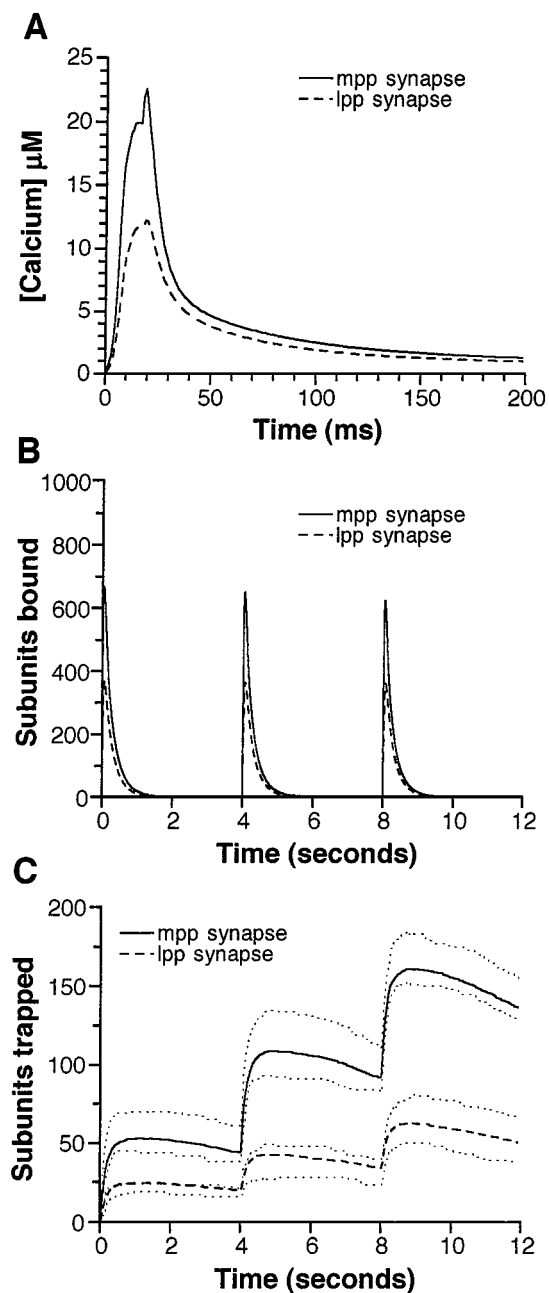


**Figure 3.** High levels of CaM $\text{Ca}_4$  binding and trapping by CaMKII are correlated with LTP induction. 300 mpp and 1 lpp synapse were activated 8 times at 400 Hz with this tetanus repeated every 4 seconds. The tetanus was assumed to coactivate shunting inhibition. Experimental data suggest that LTP is expected at the mpp synapse, but not at the lpp synapse. A: Spine head calcium concentration at mpp and lpp synapses. B: Number of CaMKII subunits with CaM $\text{Ca}_4$  bound at mpp and lpp synapses. C: Number of CaMKII subunits with CaM $\text{Ca}_4$  trapped (T<sup>286</sup> phosphorylation). The dotted lines represent extreme cases among 10 stochastic simulations and the solid and dashed lines are averages of 10 runs.

### 3.2. Frequency Dependence of Calmodulin Trapping

Simulations were done to investigate the dependence of the amount of calmodulin trapping by CaMKII on the frequency of the tetanus. Three hundred mpp synapses and one lpp synapse were activated eight times at frequencies of 400, 200, 100, 50, 20, and 10 Hz. Identical shunting inhibition was assumed in all of the simulations. Calcium concentration and CaM $\text{Ca}_4$  binding and trapping on CaMKII subunits were computed for a representative-activated mpp synapse on a dendritic spine.

It was found that reducing tetanus frequency dramatically reduced the amount of calmodulin trapping. As shown in Fig. 4A the peak spine-head calcium concentration was significantly reduced as the tetanus frequency was lowered. With the 400 Hz input, the cell fired two action potentials with the second causing the odd-shaped peak in the calcium concentration curve. With the 200 Hz stimulus, the cell fired one action potential. There were no action potentials with lower input frequencies. The different calcium signals in the six cases caused different amounts of CaM $\text{Ca}_4$  to form and bind to CaMKII subunits as shown in Fig. 4B. The 200 and 400 Hz stimuli caused similar numbers of CaMKII subunits to bind CaM $\text{Ca}_4$  (about 67% at the peak). However, as frequency was reduced to 100, 50, 20, and 10 Hz, the percentage of subunits bound with CaM $\text{Ca}_4$  at the peak fell to 60%, 50%, 20%, and 8%, respectively. This steep gradient in the amount of binding as a function of input frequency was also seen in the number of trapped subunits at the different frequencies as shown in Fig. 4C. Here the peak number of trapped subunits is 10-fold larger at 200 and 400 Hz than at 10 Hz.

### 3.3. Sensitivity of Calmodulin Trapping to the Strength of the Calcium Signal

To test the sensitivity of calmodulin trapping to changes in the calcium signal, the shunting inhibition activated by a strong input, eight-pulse, 50 Hz tetanus was reduced to one-half or one-third of the level used above. The cell fired two action potentials in the case with the lowest inhibition, one action potential in the case with intermediate level inhibition, and no action potentials with the highest level of shunting inhibition. The calcium concentration in the spine head and subsequent binding and trapping of CaM $\text{Ca}_4$  to CaMKII subunits were computed.

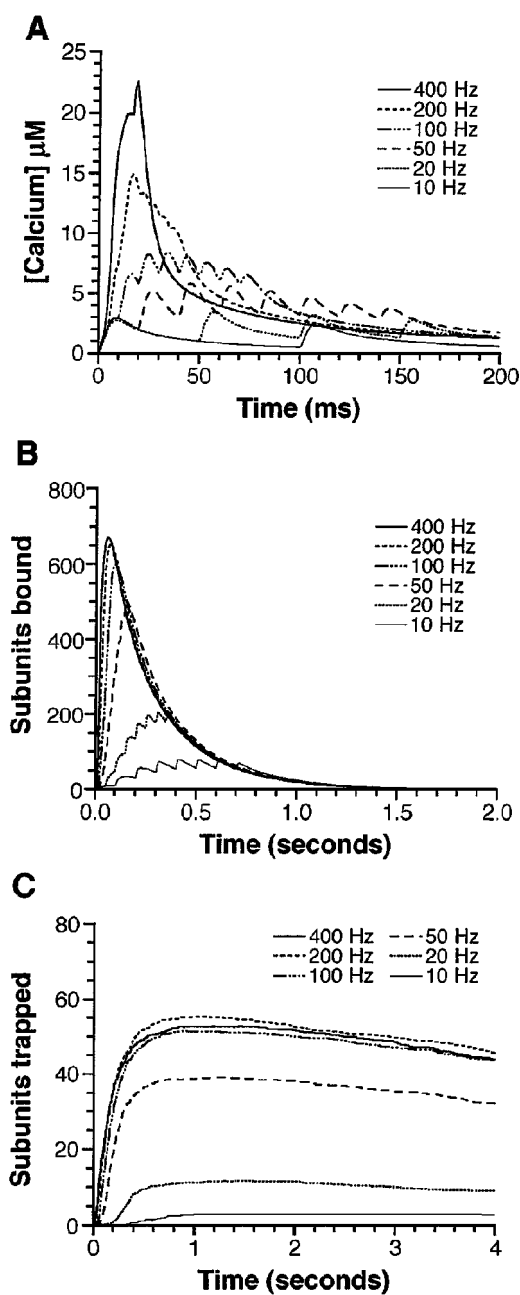


**Figure 4.** Frequency dependence of CaMCA<sub>4</sub> binding and trapping on CaMKII. 300 mpp synapses were activated 8 times at 400, 200, 100, 50, 20, and 10 Hz. A: Spine head calcium concentration. B: Number of CaMKII subunits with CaMCA<sub>4</sub> bound. C: Number of CaMKII subunits with CaMCA<sub>4</sub> trapped. Plots represent the average of 10 stochastic simulations.

Despite what might seem to be small differences in the calcium signal with reduced inhibition, there were large differences in the amount of calmodulin binding

and trapping in the three cases. The calcium concentration in the spine heads is shown in Fig. 5A. Overall, the calcium concentration curves look similar except that the peaks are elevated by 1 to 3  $\mu\text{M}$  at each pulse in the tetanus as inhibition is reduced. The elevated peak in calcium concentration at the second pulse of the tetanus in the simulation with the lowest level of inhibition is due to the action potential invading the dendrites and the dendritic spine containing the observed synapse. This relatively small difference in the calcium signal caused the peak number of subunits bound with CaMCA<sub>4</sub> to be 824, 735, and 501 in the three cases (plot not shown). This difference was further amplified into twofold to threefold differences in the amount of calmodulin trapping (Fig. 5B).

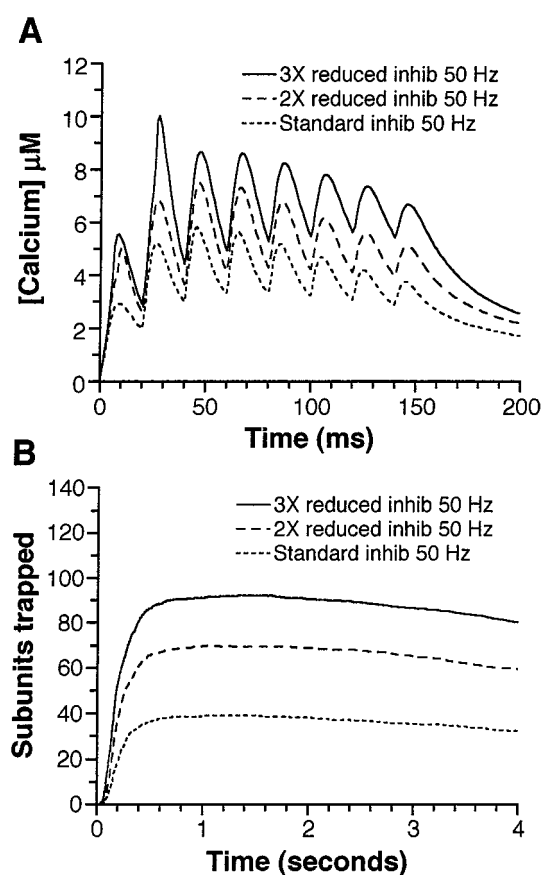


**Figure 5.** Relatively small differences in the calcium signal produce large differences in calmodulin trapping. The level of inhibition co-activated with an 8 pulse 50 Hz tetanus to 300 mpp synapses was reduced to 50% or 33% of the baseline level. A: Spine head calcium concentration. B: Number of CaMKII subunits with CaMCA<sub>4</sub> trapped (average of 10 simulations).

It should be noted that similar large differences with changes in the level of inhibition were not seen when the frequency was reduced to 20 Hz or 10 Hz (results not shown). At lower frequencies, as inhibition was reduced, we approached the case illustrated in Fig. 2 when there was no inhibition (but also no tetanus). The increased calcium signal with lower inhibition was not sufficient to provide a significant increase in the number of bound subunits at these lower tetanus frequencies.

### 3.4. Three Stages of CaMKII Activation

Calculations were done to determine the time course of CaMKII activation at mpp and lpp synapses. Comparisons were done first for a single eight-pulse 400 Hz tetanus to 300 mpp synapses and one lpp synapse and then for the tetanus applied 10 times at 10 second intervals (to simulate more closely experimental conditions used to induce LTP). Bound and trapped subunits were assigned an activation level of 1.0, and autonomous and capped subunits were assigned an activation level of 0.4 (because of their lower activity, Schulman, 1993). Total CaMKII "activation" was the weighted sum of the numbers of subunits in the different states. Results are expressed as a percentage of the maximum possible activation.

When the tetanus was applied once, three stages of CaMKII activation were observed. At each stage CaMKII activation was two to three times larger at the mpp synapse than at the lpp synapse. In the first stage 67% of the CaMKII subunits were activated at the mpp synapse and 36% were activated at the lpp synapse (Fig. 6A). Activation was highest at about 70 msec when CaM $Ca_4$  became bound to CaMKII subunits, but then fell precipitously over the next 1.0 second as calcium concentration decayed. The duration of this stage was determined by the rate constants for calcium dissociation from CaMKII-CaM $Ca_4$  and for CaM $Ca_4$  dissociation from CaMKII subunits in the bound state. In the second stage CaMKII activation decayed from 7.6% to 2.1% for the mpp synapse and from 3.3% to 0.8% for the lpp synapse (Fig. 6B). This stage began at 1.0 second when the number of trapped subunits had reached its maximum (Fig. 6C) and lasted about 40 seconds. All CaMKII activation in this period was calcium independent. The duration of this stage was determined largely by the rate constant for the transition from the trapped state to the autonomous state and to a much lesser extent by the rate of T<sup>286</sup> dephosphorylation. In the third stage, activation decayed more

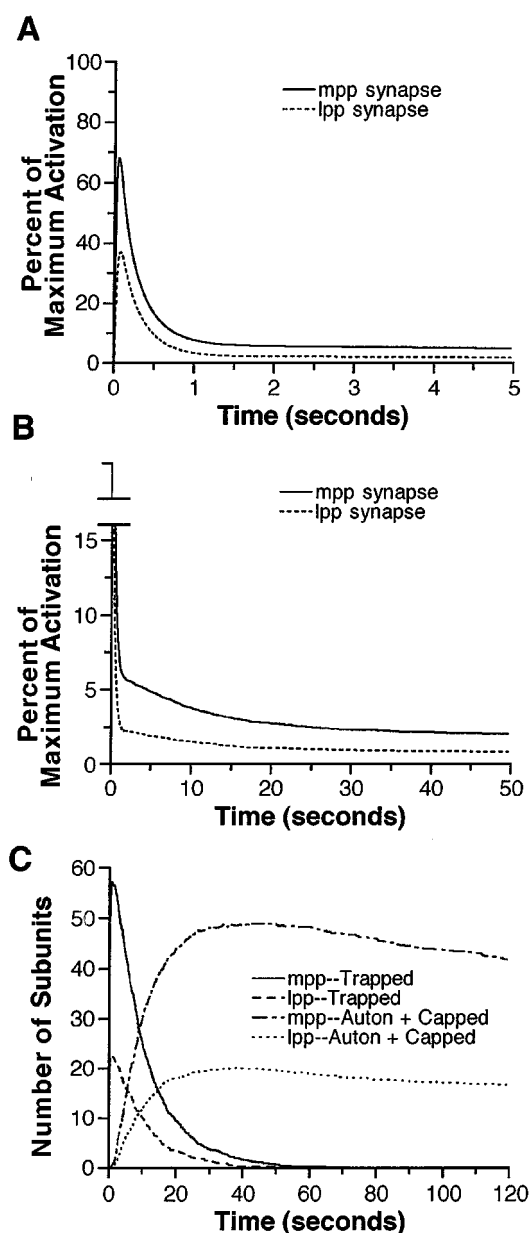


Figure 6. The time course of CaMKII activation has three stages. Simulation conditions were the same as in Fig. 3 except that the tetanus was not repeated. A: Percentage of maximum possible CaMKII activation at mpp and lpp synapses. B: Same as A but with different axes ranges to show more clearly the different stages. C: Number of subunits in the trapped and autonomous plus capped states at mpp and lpp synapses.

slowly because subunits remained in the autonomous and capped states for a long time before being dephosphorylated (Fig. 6C). This stage lasted many minutes. Few subunits reached the capped state when a single

tetanus was applied because of the requirement that the capping reaction be an intersubunit reaction. Thus the duration of the third stage depended primarily on the dephosphorylation rate constant from the autonomous state and only to a small extent on the rate constant for the transition from the autonomous to the capped state.

When the eight-pulse 400 Hz tetanus was repeated 10 times at 10 second intervals, CaMKII activation again was twofold to threefold higher at the mpp synapse than at the lpp synapse. The three stages of CaMKII activation described above appeared again in Fig. 7A. A very short-lived highly activated state was followed by a slow decay of activation between stimuli, and this was followed by a much prolonged decay of CaMKII activation after the last tetanus. Repetition of the tetanus had the effect of increasing the amplitude and duration of the prolonged third phase of CaMKII activation (Fig. 7A). At 2.5 minutes CaMKII activation was 17.2% at the mpp synapse but only 8.4% at the lpp synapse, compared to 1.6% at the mpp synapse and 0.6% at the lpp synapse when the tetanus was applied only once. This final stage of CaMKII activation lasted longer than when the tetanus was applied only once because significant numbers of subunits became capped, and intersubunit autophosphorylation tended to return autonomous subunits to the capped state (as described in the next section).

Although the prolonged phase of CaMKII activation was elevated when the tetanus was repeated, the early phase of CaMKII activation increased only slightly with the first few tetani and then decreased slightly with the last few tetani. The peak activation of the early phase was due largely to the number of bound subunits, but when the tetanus was repeated, there were fewer subunits available to enter the bound state. At the mpp synapse the peak number of bound subunits after the first tetanus was 669, but after the tenth tetanus this number was only 448. Peak activation after the tenth tetanus was still 72% due to the contribution of autonomous subunits becoming trapped. At 2.5 minutes there were 427 subunits in the autonomous and capped states at the mpp synapse (Fig. 7B), and if every other subunit were to become bound or trapped, the percentage of maximum activation would be capped at 74.4%. Thus, repeating the tetanus added to the prolonged phase of CaMKII activation while having a much smaller effect on the early phase of CaMKII activation.

The middle stage of CaMKII activation became larger with the first few tetani, but the increase became

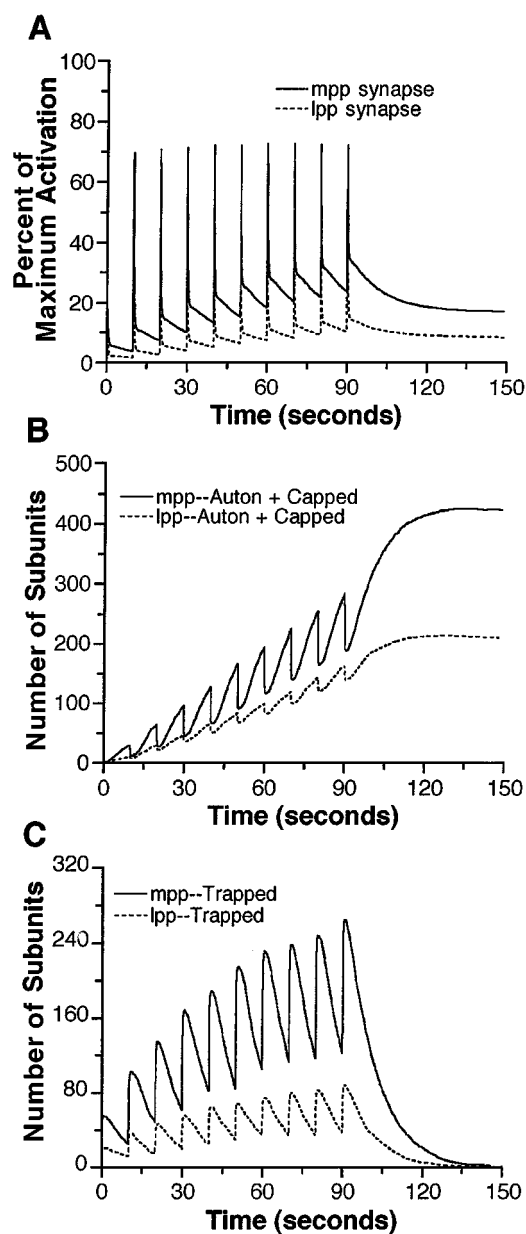


Figure 7. CaMKII activation is correlated with LTP induction conditions. Simulation conditions were the same as in Figs. 3 and 6 except that the tetanus was applied 10 times at 10 second intervals. A: Percentage of maximum possible CaMKII activation at mpp and lpp synapses. B: Number of subunits in autonomous plus capped states at mpp and lpp synapses. C: Number of subunits in the trapped state at mpp and lpp synapses.

smaller with additional tetani as the number of subunits entering the trapped state began to level off. During the first few tetani most subunits entered the trapped state

from the bound state, but by the tenth tetanus, most subunits entered the trapped state from the autonomous state (compare the amplitude of the dips in Fig. 7B with the increases in Fig. 7C). The peak number of subunits in the trapped state may have decreased if further tetani had been applied as more and more subunits became capped, limiting the available number of autonomous subunits.

### 3.5. Decay-Time Constant of CaMKII Activation

Simulations were carried out to 2 hours to examine the time course of the decay of the third stage of CaMKII activation. This stage decayed more slowly with repeated tetani than with the single tetanus. The decay-time course was fitted with a single exponential. The time constant of the decay following the single tetanus was 7 minutes at the lpp synapse and 11 minutes at the mpp synapse. However, the time constant of the decay following the repeated tetani was 27 minutes at the lpp synapse and 30 minutes at the mpp synapse. The theoretical minimum time constant is about 5 minutes (based on the assumed rate of autonomous subunit dephosphorylation). To determine the theoretical maximum decay time constant, simulations were done with all subunits starting in the capped state. The average time constant ranged from 33 to 43 minutes in five trials averaging 37 minutes. These differences in the decay-time course were a direct result of the requirement in the model that capping be an intersubunit reaction.

### 3.6. Effect of Varying Tetanus Frequency and the Interval Between Tetani

Because the above simulations illustrated the importance of repeating the tetanus, the simulations that produced the results in Fig. 7 were repeated except that the interval between tetani was reduced to 4 seconds. When this was done, the first stage of CaMKII activation was elevated to almost 85% of maximum activation at the mpp synapse (Fig. 8). Although the second stage of activation showed a similar time course of decay as before, the reduced interval between tetani allowed more subunits to become trapped. At the start of the second stage of CaMKII activation after the tenth tetanus, activation was 45% of maximum compared to 34% of maximum when the tetani were delivered at 10 second intervals. However, surprisingly, the level of activation during the third stage was nearly the same at

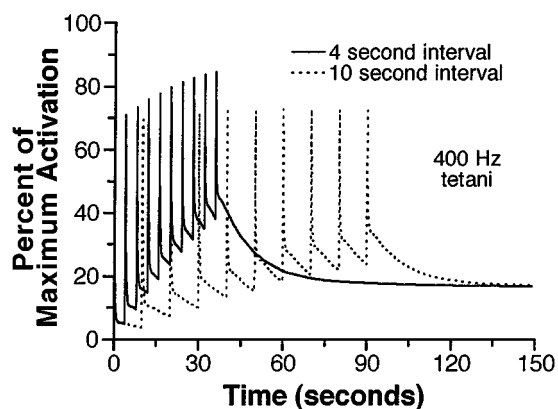
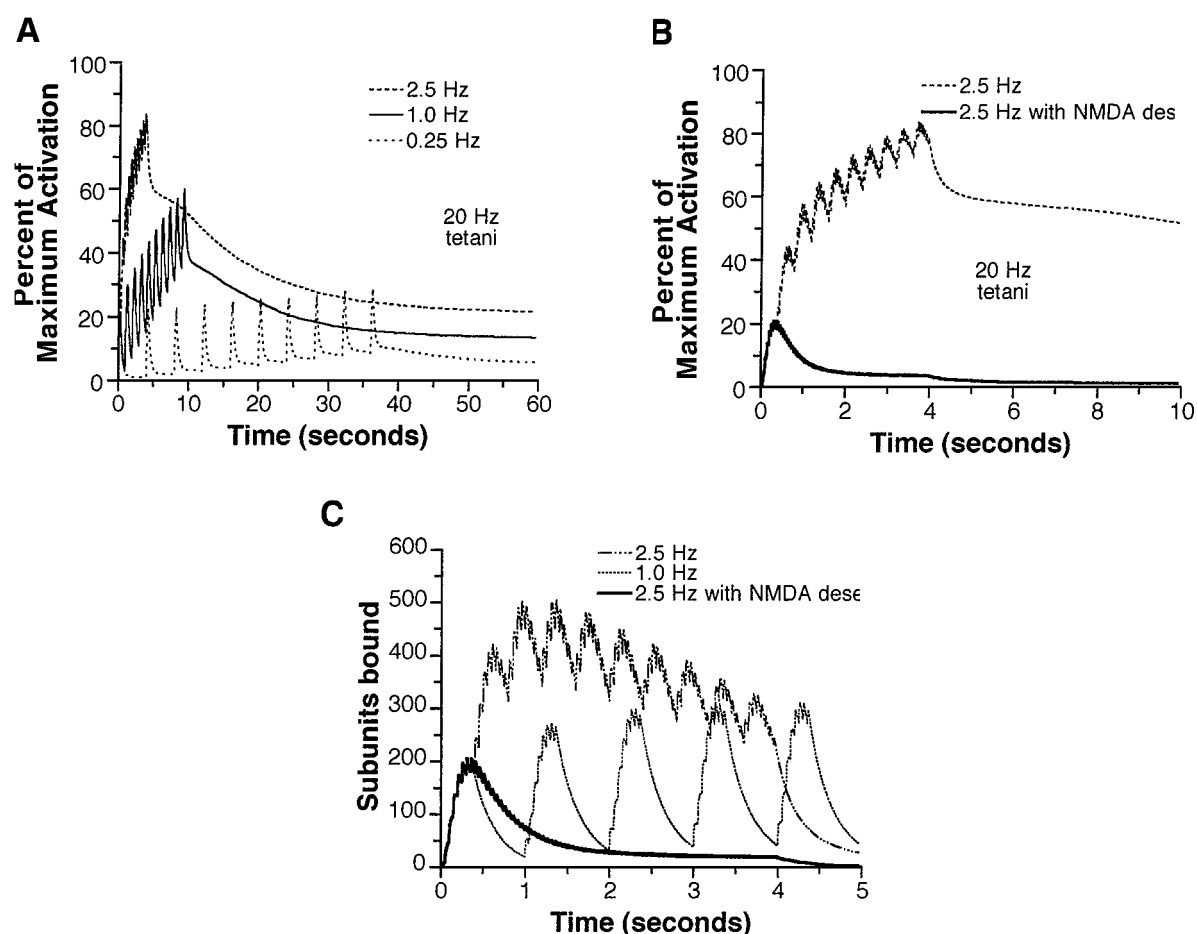


Figure 8. Effect of reducing the interval between tetani. Percentage of maximum possible CaMKII activation at the mpp synapse. Same simulation conditions as in Fig. 7 (400 Hz tetani) except that the interval between tetani was reduced to 4 seconds.

2.5 minutes whether the interval between tetani was 4 or 10 seconds; the decay time constants were also similar. If there is a difference in LTP induction between tetani delivered at 4 or 10 second intervals, then the model suggests that the difference should not lie with the third stage of CaMKII activation.

When tetani were delivered at intervals shorter than 4 seconds, recovery of NMDA receptors from desensitization between tetani became an issue. Fig. 9A shows the activation level when a 20 Hz eight-pulse tetanus was delivered 10 times at intervals of 400 ms (2.5 Hz), 1.0 second (1.0 Hz), and 4 seconds (0.25 Hz) and NMDA receptor desensitization was assumed to recover completely between tetani. In these cases there was a dramatic increase in peak CaMKII activation levels at each stage of activation as the interval between tetani was reduced. The activation level achieved when the 20 Hz tetanus was repeated at 2.5 Hz was similar to that shown in Fig. 8 for the 400 Hz tetanus repeated at 0.25 Hz. However, recovery from NMDA receptor desensitization takes much longer than the 50 ms between the last pulse of the eight-pulse 20 Hz tetanus and the first pulse of the next tetanus. When NMDA receptor kinetics were computed continuously between tetani, the level of CaMKII activation found with the 20 Hz tetanus repeated at 2.5 Hz was very low (Fig. 9B).

How NMDA receptor desensitization affects the size of the calcium signal and reduces CaMKII activation can be seen from Figs. 4A and 9C. Fig. 4A shows that the last few pulses in an eight-pulse tetanus produce smaller and smaller calcium signals. With smaller calcium signals, fewer additional subunits become bound with subsequent pulses in the tetanus (Fig. 9C). If



**Figure 9.** Recovery from NMDA receptor desensitization is important at shorter intervals between tetani. **A:** NMDA receptor desensitization was assumed to recover completely during the interval between tetani. Percentage of maximum possible CaMKII activation when a 20 Hz 8 pulse tetanus was repeated at intervals of 400 ms, 1 second, and 4 seconds (2.5, 1.0, and 0.25 Hz tetanus repetition frequencies). **B:** The lower curve represents the 2.5 Hz tetanus repetition frequency case when NMDA receptor kinetics, including desensitization and recovery from desensitization, were computed continuously throughout the inter-tetanus interval. This is compared to the 2.5 Hz case in **A** (note different time scale) where desensitization was assumed to recover completely between tetani. Note, the 2.5 Hz tetanus repetition frequency case is equivalent to a single 80 pulse 20 Hz tetanus because the interval between the last pulse of a tetanus and the first pulse of the next tetanus equals the interval between pulses within the tetanus (50 ms). **C:** Number of bound CaMKII subunits. Same set of simulations as in **A** and **B** except that the 0.25 Hz repetition frequency case has been removed for clarity.

NMDA desensitization is assumed to recover completely in the 50 ms or 650 ms interval between tetani (the 2.5 and 1.0 Hz cases in Fig. 9C), each tetanus produces the same calcium signal, there is growth (at least initially) in the peak number of subunits bound with subsequent tetani, the number of trapped subunits sums and CaMKII activation increases. However, if additional tetani are delivered before recovery from NMDA receptor desensitization, calcium signals and the peak number of bound subunits will continue to get smaller. NMDA receptor desensitization certainly is a

factor in the 2.5 Hz case (bottom curve in Fig. 9C) and may be a factor in the 1.0 Hz case.

### 3.7. Effect on the Predicted Time Course of CaMKII Activation of Different Parameter Value Choices in the Model

Although there are experimental data for many of the rate constants used in the simulations, some are not known with much certainty. Simulations were done to

examine six particular variations of the model: (1) the reactions in the dashed boxes in Fig. 1 were excluded from the model, (2) the dephosphorylation rates were increased or decreased 10-fold, (3) subunits were assumed to be autonomous or capped in the basal state, (4) the bound to trapped rate constant was increased or decreased 10-fold, (5) the autonomous to capped rate constant was reduced fivefold, and (6) the trapped to autonomous rate constant was reduced five- and 10-fold. Tests were done using 10 tetani at 10 second intervals as in Fig. 7. In all cases tested, CaMKII trapping and activation remained much larger with conditions thought to lead to LTP than with conditions thought not to lead to LTP, but some variations in parameter values caused large changes in the time course of one or more of the three stages of CaMKII activation.

### 3.7.1. Elimination of “Boxed” Reactions of Fig. 1.

Because many of the rate constants in the boxed reactions of Fig. 1 are not known well, they were eliminated from one set of simulations. Although it is usually thought that the additional reaction steps would allow CaMKII subunits to enter the bound state more easily, these reactions also allowed CaMKII subunits to leave the bound state more easily. Eliminating these reactions left only one path away from the bound state instead of two. This meant that CaMKII activation was higher than when the boxed reactions were included (Fig. 10A) because subunits remained in the bound state longer (Fig. 10B) and more became trapped (Fig. 10C). Although the rate constants for the boxed reactions are not known well, the simulation results suggest that these reactions are important to include.

### 3.7.2. Dephosphorylation Rates.

Dephosphorylation rates had profound effects on the third stage and less significant effects on the second stage of CaMKII activation. When dephosphorylation rates were reduced 10-fold only very small differences were seen in the first two stages of CaMKII activation (Fig. 11A). This occurred because the primary path out of the trapped state was to the autonomous state as determined by the trapped to autonomous rate constant when dephosphorylation rates were at the baseline levels or slower. When dephosphorylation rates were increased ten-fold, the second stage of CaMKII activation was much reduced (bottom curve in Fig. 11A). The faster dephosphorylation rate was now closer in magnitude to the trapped to autonomous rate, and this allowed dephosphorylation to become a second significant path away from the trapped state.

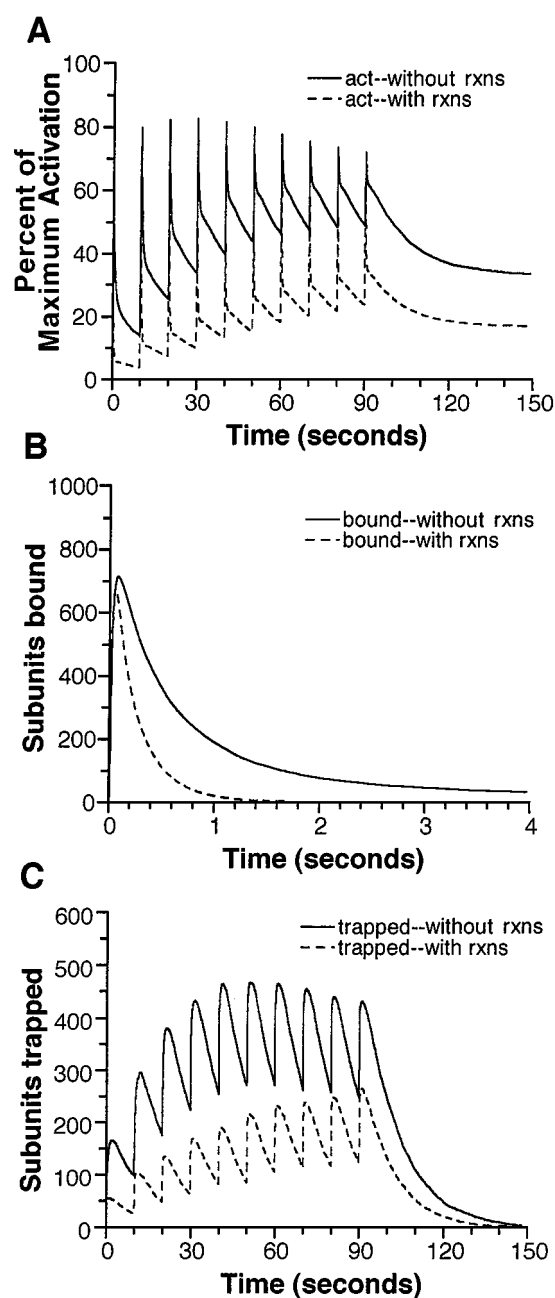


Figure 10. Effect of eliminating the “boxed” reactions in Fig. 1 from the simulations. A: Activation without the “boxed” reactions was higher because without the boxed reactions, B: subunits remained bound longer and C: more became trapped.

The large effect of dephosphorylation rates on the third stage of activation is shown in Fig. 11B, where the 150 second time period shown in Fig. 11A is extended to 2 hours. When dephosphorylation rates were reduced 10-fold, there was 20% decay of CaMKII

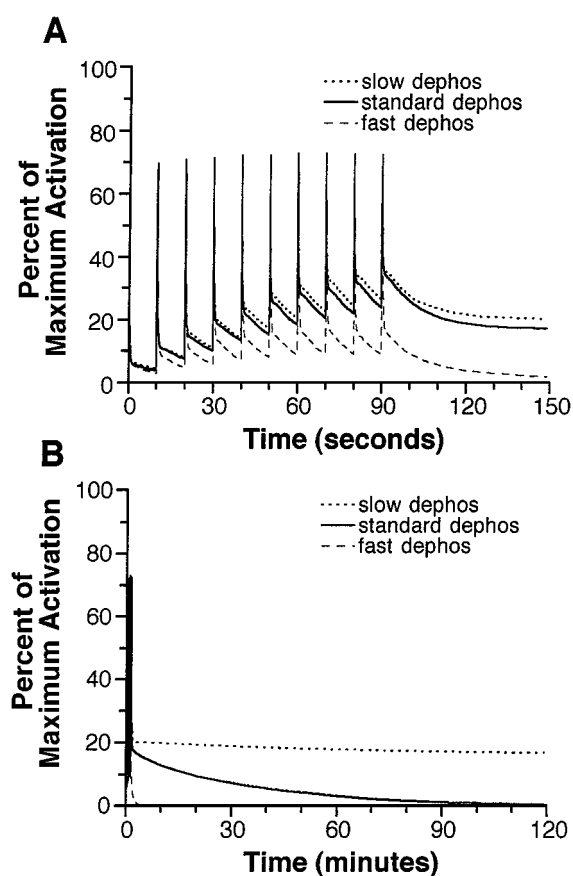


Figure 11. Differences in CaMKII activation levels and time course at the mpp synapse due to variations in dephosphorylation rates. A: Dephosphorylation rates were increased or decreased 10X. B: Same as in A except that the time scale is changed to show the third stage of CaMKII activation.

activation over 2 hours. When dephosphorylation rates were increased 10-fold, CaMKII activation was over in less than 5 minutes. Because dephosphorylation rates can depend on many factors with phosphatases regulated in a number of different ways through reaction pathways not included in this model, it was thought that any value within the 100-fold range of tested values might be appropriate at a given time.

**3.7.3. Effect of Basally Phosphorylated Subunits.** It has been reported that there is basal phosphorylation of 4% to 20% of the CaMKII subunits. To determine the effect of basally phosphorylated subunits on CaMKII activation, initial conditions were chosen from the subunit states found at 2.5 minutes in three sets of previous simulations. In these simulations approximately 4%, 12%, and 21% of the subunits were in the auto-

nomous or capped states. These initial distributions of autonomous and capped subunits were not random within a holoenzyme. Clusters of adjacent subunits were capped because of the requirement that capping be an intersubunit reaction in the simulations that created these initial conditions. Results were obtained for eight-pulse tetani of 20 Hz or 400 Hz delivered 10 times at 10 second intervals.

Surprisingly, the presence of basally phosphorylated subunits did not increase CaMKII activation significantly above the amount given by the initial condition. When the stimulus frequency was 400 Hz, the first stage of CaMKII activation was slightly reduced, and the second and third stages were slightly increased when there were basally phosphorylated subunits. The first stage was slightly reduced because there were fewer free subunits available to become bound with the calcium signal and autonomous and capped subunits had lower activation levels than bound or trapped subunits. The second and third stages were elevated by an amount corresponding to the initial condition. Having 4%, 12%, or 21% starting as autonomous or capped meant that the starting CaMKII activation was 1.6%, 4.8%, or 8.4% of the maximum level. These are the approximate differences seen in Fig. 12A. When the stimulation frequency was 20 Hz, all three stages of CaMKII activation were increased by an amount corresponding to the initial condition (Fig. 12B). Unlike the 400 Hz case, the number of subunits that became bound was not limited by the number of basally phosphorylated autonomous and capped subunits. The activation level at two minutes was 4.27% with no basal phosphorylation and was 14.1% with 21% basal phosphorylation. The difference of 9.83% is only slightly larger than the 8.4% activation given by the initial condition alone.

**3.7.4. Bound to Trapped.** The rate at which bound subunits became trapped was increased or decreased 10-fold because other models have used this range of values as mentioned in the Methods. When the bound to trapped rate constant was increased 10-fold, CaMKII activation was close to 40% following the last tetanus at both the mpp and lpp synapses. A 40% activation level is the maximum that can be attained when all subunits are in the autonomous or capped states. Because sustained CaMKII activation was nearly the same at both synapses and LTP should occur only at the mpp synapse, it was thought that the bound to trapped rate constant should not be this large. When the bound to trapped rate constant was reduced 10-fold, CaMKII

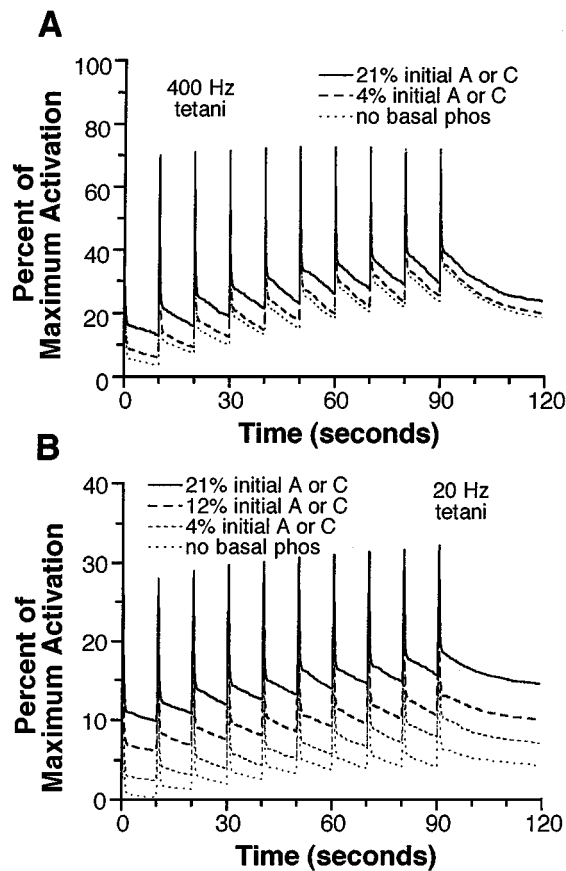


**Figure 12.** Effect of initially phosphorylated subunits on simulation results. A: 400 Hz 8 pulse tetanus was repeated 10 times at 10 second intervals. The percentage of subunits starting in the autonomous or capped states was 21%, 4%, or 0%. B: 20 Hz 8 pulse tetanus was repeated 10 times at 10 second intervals. The percentage of subunits starting in autonomous or capped states was 21%, 12%, 4%, or 0%. The initial states came from data at 2.5 minutes calculated in simulations illustrated in previous figures. Each line is the average of 4 stochastic simulations.

activation between tetani at the mpp synapse was at most 3.5% (plot not shown). During the first stage of CaMKII activation, CaMKII was nearly 70% activated, but by 1 second this had dropped significantly. Because CaMKII activation was so low at a synapse where LTP should be induced, it was thought that the rate constant should not be this small.

**3.7.5. Autonomous to Capped.** The rate of  $T^{305,306}$  autophosphorylation was reduced fivefold from the baseline value to bracket the most likely range for this rate constant. This reduction in the autonomous to capped rate constant had very little effect on the early

stages of CaMKII activation, but it did speed up the decay of the third stage of CaMKII activation by a factor of three.

**3.7.6. Trapped to Autonomous.** Slowing the transition from the trapped state to the autonomous state fivefold and 10-fold increased the peak of the first stage and lengthened the second stage of CaMKII activation. With the slower trapped to autonomous rate, the number of subunits becoming autonomous in the first 100 seconds was limited, and, consequently, the number of subunits making the transition from the autonomous to the capped state was small. With subunits primarily in the bound or trapped states, a reduction in the first stage of activation due to accumulation of capped subunits did not occur. The lengthening of the second stage of activation was expected because this stage was known to depend on this rate constant when dephosphorylation rates were at baseline levels.

## 4. Discussion

### 4.1. Correlation of CaMKII Activation with LTP Induction

The modeling results support the hypothesis that calmodulin trapping and CaMKII activation is correlated with conditions that lead to the induction of LTP. Stimulation conditions used in the model that induce LTP experimentally led to a rise in spine-head calcium concentration followed by calcium binding to calmodulin, CaM $Ca_4$  binding, and trapping on CaMKII and CaMKII activation. Stimulation conditions that do not lead to LTP experimentally caused much less CaM $Ca_4$  binding and trapping and CaMKII activation in the model.

The model results regarding calmodulin trapping by CaMKII also were consistent with three other features known or presumed about LTP. First, the results demonstrated a clear dependence of calmodulin trapping by CaMKII on the frequency of the tetanus. A steep increase in calmodulin trapping occurred as the tetanus frequency was increased from 10 to 100 Hz. Second, the extent of calmodulin trapping was extremely sensitive to the strength of the calcium signal. Small changes in the calcium signal, produced by reducing the inhibition in the model coactivated with a 50 Hz tetanus, caused huge changes in the amount of calmodulin trapping. Third, the model demonstrated the importance of repeating the short high-frequency tetanus. A

single tetanus did not produce large numbers of trapped subunits, and trapped subunits moved to the autonomous or capped states over a period of 40 seconds. However, when the tetanus was repeated at intervals much shorter than 40 seconds, such as 4 or 10 seconds, there was a significant increase in the number of trapped subunits as autonomous subunits were converted back to trapped subunits and additional free subunits became bound and then trapped. After a number of repetitions, increases in activation were small because a large number of subunits had become capped.

#### 4.2. *Frequency of Calcium Signals and CaMKII Activation*

Recently, DeKoninck and Schulman (1998) delivered pulses of  $\text{CaM}\text{Ca}_4$  to immobilized CaMKII at different frequencies and pulse widths and found that CaMKII activation was highly dependent on the frequency and duration of the  $\text{CaM}\text{Ca}_4$  pulses. They found a sharp increase in CaMKII activation as the frequency of the calcium signals was increased to the 1 to 10 Hz range. In this range many of the calcium signals had a longer duration than the interval between signals. One must be careful to distinguish between the frequency of afferent input in the model and the frequency of calcium signals. In the model each eight-pulse tetanus effectively delivered a pulse of  $\text{CaM}\text{Ca}_4$  of fixed duration, but the different tetanus frequencies delivered pulses of different sizes. The appropriate comparison to the DeKoninck and Schulman (1998) data would be to compare the change in CaMKII activation in the model as the interval between tetani was reduced.

A reduction in the interval between tetani can increase  $\text{CaM}\text{Ca}_4$  trapping on CaMKII and total CaMKII activation in two ways. The first requires the stimulus to be strong enough to get  $\text{CaM}\text{Ca}_4$  to bind to a majority of subunits. With large numbers of subunits bound, many became trapped. Repeating the stimulus after the number of trapped subunits reaches its peak (1 second in the model) but before the number of trapped subunits decays completely (40 seconds in the model) allows the number of trapped subunits to sum and total CaMKII activation to rise. Consequently, the number of trapped subunits increases as the interval between stimuli is shortened from 0.025 Hz to 1 Hz. This is what was found in the model when the strong stimulus was the eight-pulse 400 Hz tetanus and the interval between tetani was shortened from 0.1 to 0.25 Hz. The second scenario requires a weaker stim-

ulus that allows less than a majority of CaMKII subunits to bind  $\text{CaM}\text{Ca}_4$ . Repeating the stimulus between the time the number of bound subunits peaks and the time the number of bound subunits decays completely (1 to 10 Hz) allows the number of bound subunits to sum. This is what occurred in the model when the stimulus was the 20 Hz tetanus and the interval between tetani was shortened from 0.25 Hz to 2.5 Hz. However, this occurred only if NMDA receptor desensitization was assumed to recover completely between tetani. With eight-pulse tetani delivered at 1 to 10 Hz, NMDA receptor desensitization will not recover completely (Sather et al., 1992), the calcium signal will decrease with each tetanus, and the maximum number of bound subunits will remain low. This second scenario is very effective in activating CaMKII when the size of the calcium signal remains constant as it is repeated (as in the DeKoninck and Schulman experiments), but it may not be effective when the calcium signal is reduced by receptor desensitization or by channel inactivation.

#### 4.3. *Three Stages of CaMKII Activation*

The simulations suggest that there are three distinct stages of CaMKII activity following an LTP inducing stimulus—distinct stages that might be difficult to detect experimentally. The three stages have very different time courses and levels of CaMKII activation.

In the first stage CaMKII was highly activated for less than 1 second, and this activation was calcium-dependent. After a strong tetanus calcium entered the spine and bound to calmodulin and  $\text{CaM}\text{Ca}_4$  became bound to 65% to 85% of the available subunits. Peak activation coincided with the peak number of bound subunits, which occurred at 70 to 100 msec. Activity declined considerably over the next 1.0 second as  $\text{CaM}\text{Ca}_4$  was released from all subunits that did not become trapped. This short highly activated stage may have two functions. First, because  $\text{T}^{286}$  autophosphorylation is an intersubunit reaction requiring adjacent subunits to be in the bound (or other activated) state (Hanson et al., 1994), significant numbers of subunits can be autophosphorylated to the trapped state. Second, high CaMKII activity may be necessary to overcome the activity of phosphatases also activated by calcium or  $\text{CaM}\text{Ca}_4$  dependent reactions (Coussens and Teyler, 1996).

In the second stage CaMKII was moderately activated for about 40 seconds, and this activation was

calcium independent. Activity corresponded to the number of subunits that became trapped during the first stage. The number of trapped subunits peaked at about 1 second and declined relatively slowly over 40 seconds as trapped subunits lost  $\text{CaMCA}_4$  and entered the less active autonomous state. Any new calcium signal that occurred during this 40 seconds remained effective at increasing the number of trapped subunits because newly formed  $\text{CaMCA}_4$  would bind to autonomous subunits and return them to the trapped state.

In the third stage calcium-independent CaMKII activity slowly declined as autonomous and capped subunits were dephosphorylated. This stage began at about 40 seconds, and with the base set of dephosphorylation values, it could last about 2 hours. This may be related to the amount of time that a molecular tag lasts at a synapse (Frey and Morris, 1997). With other choices for the dephosphorylation rates in the simulations, this third stage of activation could last 5 minutes or many hours, illustrating the importance of phosphatase regulation (Blitzer et al., 1998).

The rate of decay of this third stage also depended on the amount of CaMKII activation. The time constant of decay ranged in the model from 5 minutes with weak activation to 45 minutes with strong activation. This difference occurred because a higher proportion of autonomous subunits became capped when activation was strong. The transition to the capped state was an intersubunit reaction requiring adjacent subunits to be activated and fewer adjacent subunits were activated with weak activation than with strong activation. The decay of weak activation depended most strongly on autonomous subunit dephosphorylation, whereas decay of strong activation depended on both autonomous and capped subunit dephosphorylation and the rate of phosphorylation to the capped state.

#### 4.4. Which Stage is Most Important for LTP?

It is not clear which stage of CaMKII activation is most important for LTP induction. Although autonomous and capped states have lower activity than bound or trapped states, the third stage might be the most important stage because of its potentially very long duration. The model suggests that a means to test this would be to assess the LTP that occurs when high-frequency tetani are delivered at different intervals. In the model there was very little difference in CaMKII activation during the third stage of activation whether the interval between tetani was 4 or 10 seconds, but there were

large differences in the level of activation at the earlier stages. If the third stage is the most important for LTP, then delivering tetani at 4 or 10 second intervals should not make a difference for LTP induction.

Interestingly, Mayford et al. (1995) have proposed that calcium-independent CaMKII activation levels may control the threshold for induction of LTP or LTD by a tetanic stimulus. High levels shift the threshold in favor of LTD. The model suggests that when calcium-independent CaMKII activity levels are high, there is loss of the first two stages of CaMKII activation because few subunits have the calmodulin binding site available for calmodulin binding. This would seem to indicate that the first two stages are important for LTP induction and the third is more important for LTD induction. It is possible, though, that new synthesis of CaMKII as has been observed after tetanic stimulation (Ouyang et al., 1997) could allow the first and second stages of CaMKII activation to be recovered.

#### 4.5. Time Course of CaMKII Phosphorylation

In recent work by Barria et al. (1997) maximum phosphorylation of CaMKII at the  $T^{286}$  site occurred at 5 minutes following an LTP inducing stimulus (although they did not measure  $T^{286}$  phosphorylation earlier than 5 minutes). The present modeling results suggest that maximum  $T^{286}$  phosphorylation (trapped plus autonomous plus capped) should occur during the first few seconds. It is difficult to see how the peak could be much later than this because the  $T^{286}$  site cannot be autophosphorylated unless  $\text{CaMCA}_4$  is bound (Brickey et al., 1994; Hanson et al., 1994) and  $\text{CaMCA}_4$  is not available to bind to additional CaMKII subunits after the first 1 to 2 seconds post-stimulus. It is possible that  $\text{CaMCA}_4$  might become available as it unbinds from other calmodulin binding proteins, but in low calcium, calcium is far more likely to unbind from  $\text{CaMCA}_4$  than for  $\text{CaMCA}_4$  to bind to CaMKII.

Barria et al. (1997) also found that the  $T^{286}$  site remained phosphorylated for 60 minutes and that total phosphorylation ( $T^{286}$  plus  $T^{305,306}$  and perhaps other sites) increased in this period. The model does not predict that the  $T^{286}$  site should remain phosphorylated this long unless dephosphorylation is very slow. With slow dephosphorylation rates the model found little decay in  $T^{286}$  phosphorylation over a period of 2 hours. Reducing the trapped to autonomous rate and increasing the autonomous to capped rate increased the duration of  $T^{286}$  phosphorylation, but the increase was small

without a reduction in the dephosphorylation rate as well. The model also does not predict an increase in total phosphorylation over 60 minutes. However, with slow dephosphorylation rates in the model, total phosphorylation peaks at 5 to 10 minutes and decreases minimally over the next 2 hours. One reason for the lack of an increase in total phosphorylation in the model is that the model only considered T<sup>286</sup> and T<sup>305,306</sup> phosphorylation and there may be other sites phosphorylated with a slower time course (e.g., Dosemeci et al., 1994).

Dephosphorylation rate constants are perhaps the most uncertain, but important, rate parameters in the model, and dephosphorylation rates may be determined not only by the activity and regulation of phosphatases (Blitzer et al., 1998), but by the location of CaMKII. For example, the rate of T<sup>286</sup> dephosphorylation may differ depending on whether CaMKII is in the cytosol or in the post-synaptic density (PSD). Although CaMKII has been thought to be a major part of the PSD (Kennedy et al., 1983; Kelly et al., 1984), a recent report suggests that CaMKII exists primarily in the cytosol and that localization at the PSD occurs as an artifactual postmortem translocation (Suzuki et al., 1994). Furthermore, it has been reported that dephosphorylation at T<sup>286</sup> is due to protein phosphatase 2A for cytosolic CaMKII and due to protein phosphatase 1 for PSD bound CaMKII (Strack et al., 1997a, 1997b). The two phosphatases may be activated by different regulatory pathways and may have different dephosphorylation rates. If dephosphorylation were rapid for cytosolic CaMKII and very slow for PSD bound CaMKII, then the mechanism of CaMKII translocation would play a key role in LTP induction. The regulation and activation of phosphatases and subsequent dephosphorylation will be left to future modeling studies once further aspects of these pathways are known.

### Acknowledgments

This work was supported by National Institute of Mental Health grant MH51081. I thank W.B. Levy and N.L. Desmond for the anatomical data of the dentate granule cell used in the simulations. I thank I. Aradi for helpful comments on the manuscript.

### References

- Barnes GN, Slevin JT, Vanaman TC (1995) Rat brain protein phosphatase 2A: An enzyme that may regulate autophosphorylated protein kinases. *J. Neurochem.* 64:340–353.
- Barria A, Muller D, Derkach V, Griffith LC, Soderling TR (1997) Regulatory phosphorylation of AMPA-type glutamate receptors by CaM-KII during long-term potentiation. *Science* 276:2042–2045.
- Bekkers JM, Stevens CF (1989) NMDA and non-NMDA receptors are co-localized at individual excitatory synapses in cultured rat hippocampus. *Nature* 341:230–233.
- Bliss TVP, Collingridge GL (1993) A synaptic model of memory: Long-term potentiation in the hippocampus. *Nature* 361:31–39.
- Blitzer RD, Connor JH, Brown GP, Wong T, Shenolikar S, Iyengar R, Landau EM (1998) Gating of CaMKII by cAMP-regulated protein phosphatase activity during LTP. *Science* 280:1940–1942.
- Brickey DA, Bann JG, Fong Y-L, Perrino L, Brennan RG, Soderling TR (1994) Mutational analysis of the autoinhibitory domain of calmodulin kinase II. *J. Biol. Chem.* 269:29047–29054.
- Burger D, Cox JA, Comte M, Stein EA (1984) Sequential conformational changes in calmodulin upon binding of calcium. *Biochemistry* 23:1966–1971.
- Burger D, Stein EA, Cox JA (1983) Free energy coupling in the interactions between Ca<sup>2+</sup>, calmodulin and phosphorylase kinase. *J. Biol. Chem.* 258:14733–14739.
- Colbran RJ (1993) Inactivation of Ca<sup>2+</sup>/calmodulin-dependent protein kinase II by basal autophosphorylation. *J. Biol. Chem.* 268:7163–7170.
- Coomber C (1998) Current theories of neuronal information processing performed by Ca<sup>2+</sup>/calmodulin-dependent protein kinase II with support and insights from computer modelling and simulation. *Computers and Chemistry* 22:251–263.
- Coussens CM, Teyler TJ (1996) Protein kinase and phosphatase activity regulate the form of synaptic plasticity expressed. *Synapse* 24:97–103.
- Cox JH, Comte M, Mamar-Bachi A, Milos M, Schaer J-J (1988) Cation binding to calmodulin and relation to function. In: Gerday C, Gilles R, Bolis L, eds. Calcium and Calcium Binding Proteins. Springer-Verlag, Berlin. pp. 141–162.
- Crouch TH, Klee CB (1980) Positive cooperative binding of calcium to bovine brain calmodulin. *Biochemistry* 19:3692–3698.
- Cummings JA, Mulkey RM, Nicoll RA, Malenka RC (1996) Ca<sup>2+</sup> signaling requirements for long-term depression in the hippocampus. *Neuron* 16:825–833.
- DeKoninck P, Schulman H (1998) Sensitivity of CaM Kinase II to the frequency of Ca<sup>2+</sup> oscillations. *Science* 279:227–230.
- Desmond NL, Levy WB (1985) Granule cell dendritic spine density in the rat hippocampus varies with spine shape and location. *Neuroscience Letters* 54:219–224.
- Dosemeci A, Albers RW (1996) A mechanism for synaptic frequency detection through autophosphorylation of CaM kinase II. *Biophys. J.* 70:2493–2501.
- Dosemeci A, Gollop N, Jaffe H (1994) Identification of a major autophosphorylation site on postsynaptic density-associated Ca<sup>2+</sup>/calmodulin-dependent protein kinase. *J. Biol. Chem.* 269:31330–31333.
- Frey U, Morris RGM (1997) Synaptic tagging and long-term potentiation. *Nature* 385:533–536.
- Fukunaga K, Muller D, Miyamoto E (1996) CaM kinase II in long-term potentiation. *Neurochem. Int.* 28:343–358.
- Fukunaga K, Stoppini L, Miyamoto E, Muller D (1993) Long-term potentiation is associated with an increased activity of

- Ca<sup>2+</sup>/calmodulin-dependent protein kinase II. *J. Biol. Chem.* 268:7863–7867.
- Gregori L, Gillevet PM, Doan P, Chau V (1985) Mechanisms of enzyme regulation by calmodulin and Ca<sup>2+</sup>. *Curr. Top. Cell. Regul.* 27:447–454.
- Hanse E, Gustafsson B (1992) Long-term potentiation and field EPSPs in the lateral and medial perforant paths in the dentate gyrus in vitro: A comparison. *Eur. J. Neurosci.* 4:1191–1201.
- Hansel C, Artola A, Singer W (1996) Different threshold levels of postsynaptic [Ca<sup>2+</sup>]<sub>i</sub> have to be reached to induce LTP and LTD in neocortical pyramidal cells. *J. Physiol. (Paris)* 90:317–319.
- Hanson PI, Meyer T, Stryer L, Schulman H (1994) Dual role of calmodulin in autophosphorylation of multifunctional CaM kinase may underlie decoding of calcium signals. *Neuron* 12:943–956.
- Hanson PI, Schulman H (1992) Inhibitory autophosphorylation of multifunctional Ca<sup>2+</sup>/calmodulin-dependent protein kinase analyzed by site-directed mutagenesis. *J. Biol. Chem.* 267:17216–17224.
- Hessler NA, Shirke AM, Malinow R (1993) The probability of transmitter release at a mammalian central synapse. *Nature* 366:569–572.
- Holmes WR (1990) Is the function of dendritic spines to concentrate calcium? *Brain Res.* 519:338–342.
- Holmes WR (1995) Modeling the effect of glutamate diffusion and uptake on NMDA and non-NMDA receptor saturation. *Biophys. J.* 69:1734–1747.
- Holmes WR, Levy WB (1990) Insights into associative long-term potentiation from computational models of NMDA receptor-mediated calcium influx and intracellular calcium concentration changes. *J. Neurophysiol.* 63:1148–1168.
- Holmes WR, Levy WB (1997) Quantifying the role of inhibition in associative long-term potentiation in dentate granule cells with computational models. *J. Neurophysiol.* 78:103–116.
- Kakiuchi S, Yasuda S, Yamazaki R, Teshima Y, Kanda K, Kakiuchi R, Sobue K (1982) Quantitative determinations of calmodulin in the supernatant and particulate fractions of mammalian tissues. *J. Biochem.* 92:1041–1048.
- Kelly PT, McGuinness TL, Greengard P (1984) Evidence that the major postsynaptic density protein is a component of a Ca<sup>2+</sup>/calmodulin-dependent protein kinase. *Proc. Natl. Acad. Sci. USA* 81:945–949.
- Kennedy MB, Bennett MK, Erondy NE (1983) Biochemical and immunochemical evidence that the “major postsynaptic density protein” is a subunit of a calmodulin-dependent protein kinase. *Proc. Natl. Acad. Sci. USA* 80:7357–7361.
- Klee CB (1988) Interaction of calmodulin with Ca<sup>2+</sup> and target proteins. In: Cohen P, Klee CB, eds. *Calmodulin*. Elsevier, Amsterdam. pp. 35–56.
- Kretsinger RH (1981) Mechanisms of selective signalling by calcium. *Neurosci. Res. Prog. Bull.* 19(3):213–328.
- Linse S, Forsen S (1995) Determinants that govern high-affinity calcium binding. *Adv. Second Mess. Phos. Res.* 30:89–151.
- Linse S, Helmersson A, Forsen S (1991) Calcium binding to calmodulin and its globular domains. *J. Biol. Chem.* 266:8050–8054.
- Lisman J (1989) A mechanism for the Hebb and the anti-Hebb processes underlying learning and memory. *Proc. Natl. Acad. Sci. USA* 86:9574–9578.
- Lisman J (1994) The CaM kinase II hypothesis for the storage of synaptic memory. *Trends Neurosci.* 17:406–412.
- Lisman J, Malenka RC, Nicoll RA, Malinow R (1997) Learning mechanisms: The case for CaM-KII. *Science* 276:2001–2002.
- Luby-Phelps K, Hori M, Phelps JM, Won D (1995) Ca<sup>2+</sup>-regulated dynamic compartmentalization of calmodulin in living smooth muscle cells. *J. Biol. Chem.* 270:21532–21538.
- Malenka RC (1991) The role of postsynaptic calcium in the induction of long-term potentiation. *Mol. Neurobiol.* 5:289–295.
- Malenka RC, Nicoll RA (1993) NMDA-receptor-dependent synaptic plasticity: Multiple forms and mechanisms. *Trends Neurosci.* 16:521–527.
- Matsushita T, Moriyama S, Fukai T (1995) Switching dynamics and the transient memory storage in a model enzyme network involving Ca<sup>2+</sup>/calmodulin-dependent protein kinase II in synapses. *Biol. Cybern.* 72:497–509.
- Mayer ML, Westbrook GL, Guthrie PB (1984) Voltage-dependent block by Mg<sup>2+</sup> of NMDA responses in spinal cord neurones. *Nature* 309:261–263.
- Mayford M, Wang J, Kandel ER, O’Dell TJ (1995) CaMKII regulates the frequency-response function of hippocampal synapses for the production of both LTD and LTP. *Cell* 81:891–904.
- Meyer T, Hanson PI, Stryer L, Schulman H (1992) Calmodulin trapping by calcium-calmodulin-dependent protein kinase. *Science* 256:1199–1202.
- Michelson S, Schulman H (1994) CaM kinase: A model for its activation and dynamics. *J. Theor. Biol.* 171:281–290.
- Miller SG, Kennedy MB (1986) Regulation of brain type II Ca<sup>2+</sup>/calmodulin-dependent protein kinase by autophosphorylation: A Ca<sup>2+</sup>-triggered molecular switch. *Cell* 44:861–870.
- Miller SG, Patton BL, Kennedy MB (1988) Sequences of autophosphorylation sites in neuronal type II CaM kinase that control Ca<sup>2+</sup>-independent activity. *Neuron* 1:593–604.
- Mukherji S, Soderling TR (1994) Regulation of Ca<sup>2+</sup>/Calmodulin-dependent protein kinase II by inter- and intrasubunit-catalyzed autophosphorylations. *J. Biol. Chem.* 269:13744–13747.
- Ouyang Y, Kantor D, Harris KM, Schuman EM, Kennedy MB (1997) Visualization of the distribution of autophosphorylated calcium/calmodulin-dependent protein kinase II after tetanic stimulation in the CA1 area of the hippocampus. *J. Neurosci.* 17:5416–5427.
- Patton BL, Miller SG, Kennedy MD (1990) Activation of type II calcium/calmodulin-dependent protein kinase by Ca<sup>2+</sup>/calmodulin is inhibited by autophosphorylation of threonine within the calmodulin-binding domain. *J. Biol. Chem.* 265:11204–11212.
- Rosenmund C, Clements JD, Westbrook GL (1993) Nonuniform probability of glutamate release at a hippocampal synapse. *Science* 262:754–757.
- Sather W, Dieudonne S, MacDonald JF, Ascher P (1992) Activation and desensitization of N-methyl-D-aspartate receptors in nucleated outside-out patches from mouse neurones. *J. Physiol.* 450:643–672.
- Schulman H (1993) The multifunctional Ca<sup>2+</sup>/calmodulin-dependent protein kinases. *Curr. Opin. Cell. Biol.* 5:247–253.
- Sharma RK, Mooibroek M, Wang JH (1988) Calmodulin-stimulated cyclic nucleotide phosphodiesterase isozymes. In: Cohen P, Klee CB, eds. *Calmodulin*. Elsevier, Amsterdam. pp. 265–295.
- Silver RA, Traynelis SF, Cull-Candy SG (1992) Rapid-time-course miniature and evoked excitatory currents at cerebellar synapses in situ. *Nature* 355:163–166.

- Soderling TR (1993) Calcium/calmodulin-dependent protein kinase II: Role in learning and memory. *Mol. Cell. Biochem.* 127:128:93–101.
- Staley KJ, Mody I (1991) Integrity of perforant path fibers and the frequency of action potential independent excitatory and inhibitory synaptic events in dentate gyrus granule cells. *Synapse* 9:219–224.
- Stemmer PM, Klee CB (1994) Dual calcium ion regulation of calcineurin by calmodulin and calcineurin B. *Biochemistry* 33:6859–6866.
- Strack S, Barban MA, Wadzinski BE, Colbran RJ (1997a) Differential inactivation of postsynaptic density-associated and soluble Ca<sup>2+</sup>/calmodulin-dependent protein kinase II by protein phosphatases 1 and 2A. *J. Neurochem.* 68:2119–2128.
- Strack S, Choi S, Lovinger DM, Colbran RJ (1997b) Translocation of autophosphorylated calcium/calmodulin-dependent protein kinase II to the postsynaptic density. *J. Biol. Chem.* 272:13467–13470.
- Stull JT (1988) Myosin light chain kinases and caldesmon: biochemical properties and roles in skeletal and smooth muscle contractions. In: Cohen P, Klee CB, eds. *Calmodulin*. Elsevier, Amsterdam. pp. 91–122.
- Suzuki T, Okumura-Noji K, Tanaka R, Tada T (1994) Rapid translocation of cytosolic Ca<sup>2+</sup>/calmodulin-dependent protein kinase II into postsynaptic density after decapitation. *J. Neurochem.* 63:1529–1537.
- Walmsley B, Edwards FR, Tracey DJ (1988) Nonuniform release probabilities underlie quantal synaptic transmission at a mammalian excitatory central synapse. *J. Neurophysiol.* 60:889–908.
- White G, Levy WB, Steward O. (1988) Evidence that associative interactions between synapses during the induction of long-term potentiation occur within local dendritic domains. *Proc. Natl. Acad. Sci. USA* 85:2368–2372.
- White G, Levy WB, Steward O (1990) Spatial overlap between populations of synapses determines the extent of their interaction during the induction of long-term potentiation and depression. *J. Neurophysiol.* 64:1186–1198.
- Zador A, Koch C, Brown TH (1990) Biophysical model of a Hebbian synapse. *Proc. Natl. Acad. Sci. USA* 87:6718–6722.